Umeå University

DiVA✦

http://umu.diva-portal.org

© 2012 Society for Industrial and Applied Mathematics

WEAK MATERIAL APPROXIMATION OF HOLES WITH TRACTION-FREE BOUNDARIES[*]

MARTIN BERGGREN[†] AND FOTIOS KASOLIS[‡]

Abstract. Consider the solution of a boundary-value problem for steady linear elasticity in which the computational domain contains one or several holes with traction-free boundaries. The presence of holes in the material can be approximated using a weak material; that is, the relative density of material ρ is set to $0 < \epsilon = \rho \ll 1$ in the hole region. The weak material approach is a standard technique in the so-called material distribution approach to topology optimization, in which the inhomogeneous relative density of material is designated as the design variable in order to optimize the spatial distribution of material. The use of a weak material ensures that the elasticity problem is uniquely solvable for each admissible value $\rho \in [\epsilon, 1]$ of the design variable. A finite-element approximation of the boundary-value problem in which the weak material approximation is used in the hole regions can be viewed as a nonconforming but convergent approximation of a version of the original problem in which the solution is continuously and elastically extended into the holes. The error in this approximation can be bounded by two terms that depend on ϵ. One term scales linearly with ϵ with a constant that is independent of the mesh size parameter h but that depends on the surface traction required to fit elastic material in the deformed holes. The other term scales like $\epsilon^{1/2}$ times the finite-element approximation error inside the hole. The condition number of the weak material stiffness matrix scales like ϵ^{-1}, but the use of a suitable left preconditioner yields a matrix with a condition number that is bounded independently of ϵ. Moreover, the preconditioned matrix admits the limit value $\epsilon \to 0$, and the solution of corresponding system of equations yields in the limit a finite-element approximation of the continuously and elastically extended problem.

Key words. FEM, linear elasticity, material distribution approach, topology optimization, fictitious domain methods, preconditioning, surface traction

AMS subject classifications. 35Q74, 65N30, 65N85, 74B05, 74S05, 74P15

DOI. 10.1137/110835384

1. Introduction. Numerical design optimization has evolved into an increasingly useful tool that complements traditional methods in the engineering design of mechanical components. Such optimization can be carried out at various levels of generality. The most general case admits topological properties, such as the number of holes in the configuration, to vary during the optimization procedure; the term *topology optimization* is often used in order to highlight the generality. Perhaps the most common way of carrying out numerical topology optimization of linear elastic continua is through the *material distribution method*. In this method, the presence or absence of material is represented by an inhomogeneous relative density appearing in the coefficients of the elasticity equations, discretized on a fixed, typically uniform, mesh. This method has developed into something of a success story and is increasingly used in the design of advanced mechanical components, particularly in the automotive and aeronautical industries. For instance, three applications of topology optimization carried out on the Airbus A380 aircraft is estimated to have contributed to weight savings in the order of 1000 kg per aircraft [15].

[†]Corresponding author. Department of Computing Science, Umeå University, SE–901 87 Umeå, Sweden (martin.berggren@cs.umu.se).

[‡]Department of Computing Science, Umeå University, SE–901 87 Umeå, Sweden (fotios.kasolis@cs.umu.edu).

The idea of finding the geometry of an object by numerically optimizing over a characteristic function goes back at least to the 1973 article by Céa, Gioan, and Michel [8], which treated a scalar elliptic problem. For linear elasticity, numerical realizations of this idea was pursued in a seminal paper by Bendsøe and Kikuchi [3], published in 1988. Bendsøe and Sigmund [4] provide a current comprehensive introduction to topology optimization techniques and applications, and Allaire [2] thoroughly covers the mathematical context from the viewpoint of homogenization theory.

As detailed in section 5, when using the standard variational form of the elasticity equations, a hole with traction-free boundary conditions can be created simply by removing the hole volume from the integration in the variational form. This approach corresponds to imposing a vanishing relative density of material in the hole region. Thus, a zero-or-one relative density of material can be used as a *material indicator* to specify presence and absence, respectively, of material with a traction-free boundary condition at the interface between material and nonmaterial (void).

However, the use of a binary, 0-1 material indicator is not practical for several reasons. First, this approach leads typically to a mathematical problem that is ill posed. Second, to enable the use of gradient-based optimization methods, it is preferable to allow the relative density to attain values in a continuum between zero and one and use penalty to force the density to attain "almost" binary values.[1] Third, in order to avoid a singular stiffness matrix in the regions of vanishing density and to make the problem solvable everywhere in the design domain, it is standard practice to use a small but nonzero relative density to approximate the void region, a strategy known as the *weak material approximation*.

The weak material approach is computationally convenient to employ when implementing the material distribution approach to topology optimization: the problem size becomes fixed independent of the shapes and number of holes in the domain, and the stiffness matrix will always be nonsingular. The folklore in the community as well as our own computational experience indicate that the approach in many cases "works fine," in the sense that the solution does not seem to be particularly sensitive to the value of the lower positive bound of the density, at least for the standard problem of so-called compliance minimization. Nevertheless, it is natural to ask for a more quantitative appraisal of the weak material approach.

Perhaps surprisingly, there is not much published analysis of the effect of the weak material approximation of void. The weak material approach can be viewed as an instance of a *fictitious domain* or *domain embedding* method, in which the computations are performed on a larger "fictitious" domain that embeds the domain of interest. Fictitious domain methods that essentially correspond to the weak material approach in topology optimization have been proposed and analyzed for scalar elliptic problems by Glowinski and Pan [10], Glowinski et al. [11], and Zhang [22]. Using a lower bound of $\epsilon > 0$ for the relative density level, these articles prove $O(\epsilon^{1/2})$ convergence rates in the context of a finite-element discretization [10, 11], and an $O(\epsilon)$ convergence rate without discretization [22].

The problem of optimizing the layout of a network of truss elements is a discrete counterpart to the topology optimization problem for continuum elastic structures. The analogue to the weak material approach for truss structures is the use of truss elements with small but nonzero cross-sectional areas to approximate the complete

---

[1]The use of a continuous but penalized density usually leads to an ill-posed optimization problem that needs to be regularized in order to obtain usable results. Borrvall [5] discusses and compares many of the various regularization procedures that have been proposed.

removal of elements. In contrast to the elasticity case, the effects of the lower bound on cross-sectional areas for truss network optimization has been subject to quite extensive analysis [1], [9, Appendix 2], [14, Appendix 2], [16, 18, 19, 20]. Our hope is that the analysis presented in this article will constitute a first step towards such an analysis also in the context of topology optimization for continuum elastic structures.

In the present article we show that a finite-element approximation of the linear elasticity equations using the weak material approximation of void can be viewed as a nonconforming, convergent approximation of an elastically extended version of the original problem. In the extended problem, the displacement field inside the holes are defined as the continuous elastic extension of the outside displacement field. Theorem 8.3 proves, for a fixed mesh size h, an $O(\epsilon^{1/2})$ error bound for the weak material finite-element approximation, in accordance with previous results for scalar elliptic problems [10, 11]. Moreover, Theorem 8.3 also proves a stronger $O(\epsilon)$ error bound in the limit $h \to 0$, in accordance with the result of Zhang [22] for scalar elliptic problems. In addition, we show that the condition number of the stiffness matrix using the weak material approximation scales like ϵ^{-1}, which limits the usefulness of the convergence result above. However, we also show how the stiffness matrix can be preconditioned so that the condition number will be bounded independently of ϵ. Moreover, this preconditioned matrix admits the limit value $\epsilon \to 0$, and the corresponding solution then becomes the elastically extended solution mentioned above.

2. Preliminaries. Let Ω be an open and bounded domain in $\mathbb{R}^d$, $d = 2$, 3, with a Lipschitz boundary $\partial\Omega$; that is, the boundary is locally the graph of a Lipschitz function [12, Def. 1.2.1.1]. We denote by $H^m(\Omega)$ the Sobolev space of nonnegative integer order m; that is, $H^m(\Omega)$ is the space of functions on Ω in which each function and all its weak partial derivatives up to order m are square integrable over Ω, and we will denote the norm of a function $v \in H^m(\Omega)$ by $\|v\|_{m,\Omega}$. Thus, $H^0(\Omega) = L^2(\Omega)$, the space of square-integrable functions. Moreover, the $H^m(\Omega)$ seminorm is denoted $|v|_{m,\Omega}$ and satisfies $\|v\|_{m,\Omega}^2 = \|v\|_{0,\Omega}^2 + |v|_{m,\Omega}^2$.

The *trace* γv of a function $v \in H^1(\Omega)$ generalizes the concept of *restriction* $v|_{\partial\Omega}$ of a smooth function v to the boundary. That is, $\gamma v = v|_{\partial\Omega}$ when $v \in C(\overline{\Omega}) \cap H^1(\Omega)$, but the trace is well defined for each $v \in H^1(\Omega)$, including those that are not pointwise continuous. The range of the trace operator γ when the domain spans $H^1(\Omega)$ can be identified as the Sobolev space $H^{1/2}(\partial\Omega)$, equipped with the norm

$$(2.1) \qquad \|g\|_{1/2,\partial\Omega}^2 = \int_{\partial\Omega} g^2 + \int_{\partial\Omega_{\boldsymbol{x}} \times \partial\Omega_{\boldsymbol{y}}} \frac{[g(\boldsymbol{x}) - g(\boldsymbol{y})]^2}{|\boldsymbol{x} - \boldsymbol{y}|^d}.$$

Remark 2.1. In this article, we suppress the measure symbol (such as $\mathrm{d}x$) in all integrals. The kind of measure used in the integrals will be clear from the domain of integration. $\square$

The trace operator is a bounded linear operator from $H^1(\Omega)$ to $H^{1/2}(\partial\Omega)$ [21, Thm. 8.7]; that is, there is a constant C such that

$$(2.2) \qquad \|\gamma v\|_{1/2,\partial\Omega} \le C\|v\|_{1,\Omega} \quad \forall v \in H^1(\Omega).$$

Moreover, γ has a continuous right inverse γ^* [21, Thm. 8.8]; that is, there is a linear mapping $\gamma^* : H^{1/2}(\partial\Omega) \to H^1(\Omega)$ such that for each $g \in H^{1/2}(\partial\Omega)$, $\gamma\gamma^*g = g$, and there is a constant C such that

$$(2.3) \qquad \|\gamma^*g\|_{1,\Omega} \le C\|g\|_{1/2,\partial\Omega} \quad \forall g \in H^{1/2}(\partial\Omega).$$

The inverse trace theorem [21, Thm. 8.8] establishes the existence of a right inverse. However, the right inverse is not unique. A particular right inverse that we will use is the *minimum-norm extension* $\mathcal{X} : H^{1/2}(\partial\Omega) \to H^1(\Omega)$; that is, given $g \in H^{1/2}(\partial\Omega)$, we define $\mathcal{X}g = u$, where $u \in H^1(\Omega)$ satisfies $\gamma u = g$ and

$$(2.4) \qquad \|u\|_{1,\Omega} \leq \|v\|_{1,\Omega} \quad \forall v \in H^1(\Omega) \text{ such that } \gamma v = g.$$

Expressions (2.3) and (2.4) imply that

$$(2.5) \qquad \|\mathcal{X}g\|_{1,\Omega} \leq \|\gamma^* g\|_{1,\Omega} \leq C\|g\|_{1/2,\partial\Omega}$$

for the same C as in inequality (2.3).

The trace γ_Γ on a measurable open subset $\Gamma \subset \partial\Omega$ of the boundary is defined by restricting the range of γ and the domain of integration in (2.1). Inequality (2.2) then yields the bound

$$(2.6) \qquad \|\gamma_\Gamma v\|_{1/2,\Gamma} \leq C\|v\|_{1,\Omega} \quad \forall v \in H^1(\Omega)$$

for the same constant C as in trace inequality (2.2). We will not need to employ right inverses of the partial trace γ_Γ.

The notation $\langle \lambda, g \rangle_{1/2,\partial\Omega}$ will be used for a bounded linear functional λ operating on $g \in H^{1/2}(\partial\Omega)$. The space of bounded linear functionals on $H^{1/2}(\partial\Omega)$ is denoted by $H^{-1/2}(\partial\Omega)$ and is equipped with the induced norm

$$(2.7) \qquad \|\lambda\|_{-1/2,\partial\Omega} = \sup_{\substack{g \in H^{1/2}(\partial\Omega) \\ g \neq 0}} \frac{1}{\|g\|_{1/2,\partial\Omega}} \langle \lambda, g \rangle_{1/2,\partial\Omega}.$$

Vectors (in the sense of first-order tensors) in $\mathbb{R}^d$ will be denoted by boldface italic letter, $\boldsymbol{u}$, $\boldsymbol{v}$, and their Cartesian components by u_i, v_i, $i = 1, \ldots, d$. The space of vector-valued functions in which each component is in a Sobolev space X will be denoted by $\boldsymbol{X}$. Moreover, the action of any of the above-defined operators associated with boundary traces $(\gamma, \gamma_\Gamma, \gamma^*, \mathcal{X})$ on vector-valued functions is defined through its action on each component, and we will not distinguish with symbols the cases when these operators act on scalar- versus vector-valued functions.

3. The elasticity problem in differential form. We consider a case, schematically illustrated in Figure 3.1, in which the *ground structure* $\hat{\Omega}$ is an open, bounded, and simply connected point set in $\mathbb{R}^d$, $d = 2$ or 3. We introduce a hole $\omega \subset \hat{\Omega}$ (strict inclusion), which also is an open and simply connected point set. We wish to solve a boundary-value problem for linear elasticity on the nonsimply connected domain $\Omega = \hat{\Omega} \setminus \overline{\omega}$ using traction-free boundary conditions at the hole boundaries, whereas the rest of the boundary is partially fixed and partially subject to a prespecified traction. The generated domain Ω will be connected due to the strict inclusion of ω in Ω, and we assume that the boundary of Ω is Lipschitz. Everything below can be generalized to a setup with multiple holes, such as the domain illustrated in Figure 3.2, but in order to keep the notation simple and to clearly expose the ideas, we restrict the attention to the simpler case of Figure 3.1.

Let $\boldsymbol{u} : \overline{\Omega} \to \mathbb{R}^d$ denote the displacement field defined on $\overline{\Omega}$, $\boldsymbol{n}$ the outward-directed unit normal vector field defined almost everywhere on $\partial\Omega$, and $\boldsymbol{\sigma} : \overline{\Omega} \to \mathbb{R}^{d^2}$
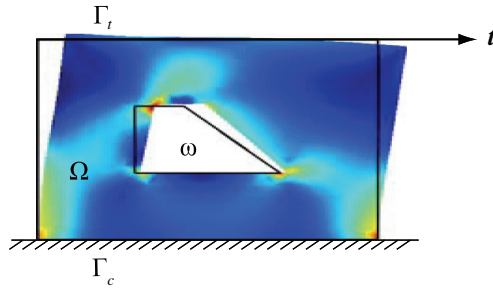
FIG. 3.1. *The model setup consists of an elastic structure containing a hole ω. A portion Γ_c of the outer boundary is fixed in space, another portion Γ_t of the outer boundary is subject to a nonzero surface traction $\boldsymbol{t}$, and the rest of the boundaries are subject to a vanishing surface traction.*
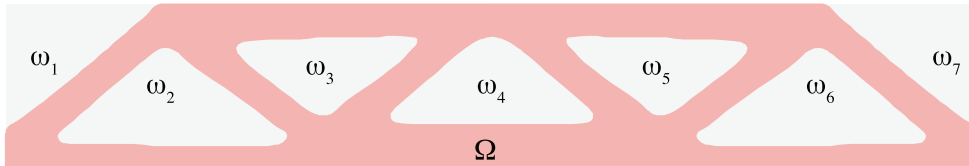

FIG. 3.2. *An example domain with multiple holes typical for topology optimization problems. The ground structure $\hat{\Omega}$ is the rectangular union of the shaded area Ω and the gray holes $\omega_1, \ldots, \omega_7$.*

the stress tensor field. In a loading case like the one illustrated in Figure 3.1, the equilibrium state of the elastic body is governed by the equations

(3.1)
$$\begin{aligned} \nabla \cdot \boldsymbol{\sigma} &= \boldsymbol{0} \quad \text{in } \Omega, \\ \boldsymbol{u} &= \boldsymbol{0} \quad \text{on } \Gamma_c, \\ \boldsymbol{\sigma n} &= \boldsymbol{0} \quad \text{on } \partial\omega, \\ \boldsymbol{\sigma n} &= \boldsymbol{t} \quad \text{on } \Gamma_t = \partial\Omega \setminus (\Gamma_c \cup \partial\omega), \end{aligned}$$

where $\boldsymbol{t}$ is the applied surface traction on the structure. Thus, the surface traction is zero on the boundary of the hole, but it may be nonzero on part of the rest of the boundary. We assume that the portion of the boundary Γ_c where the structure is clamped carries a positive $(d-1)$-dimensional measure, that is, that

(3.2)
$$\int_{\Gamma_c} > 0.$$

Under the assumptions of linear elasticity, the stress tensor and the displacement field are related through Hooke's law,

(3.3)
$$\boldsymbol{\sigma} = \boldsymbol{E}\nabla\boldsymbol{u},$$

or in Cartesian components, using Einstein's summation convention,[2]

(3.4)
$$\sigma_{ij} = E_{ijkl}\frac{\partial u_k}{\partial x_l},$$

---

[2]That is, summation from 1 to d over repeated indices.

where $\boldsymbol{E}$ is the fourth-order elasticity tensor, satisfying standard conditions on symmetry and positive definiteness (as discussed, for instance, by Gurtin [13, sect. 29]):

$$E_{ijkl} = E_{jikl}, \quad E_{ijkl} = E_{klij}$$

(3.5) $\quad \exists \alpha > 0$ such that

$$\alpha |\boldsymbol{\tau}|^2 \leq \boldsymbol{\tau} \cdot \boldsymbol{E}\boldsymbol{\tau} \text{ for each symmetric second-order tensor } \boldsymbol{\tau}.^3$$

If the material is inhomogeneous, we require that $E_{ijkl} \in L^\infty(\hat{\Omega})$ and that conditions (3.5) are satisfied uniformly almost everywhere in $\hat{\Omega}$. Note that the elasticity tensor is assumed to be defined, bounded, and satisfying conditions (3.5) also in the hole region ω!

Remark 3.1. The exact structure of $\boldsymbol{E}$, which is not important for the discussion here, depends on the constitutive properties of the material in question. In the simplest case, a homogeneous and isotropic elastic material, the action of the elasticity tensor can be written

$$(3.6) \qquad \boldsymbol{E}\nabla\boldsymbol{u} = \lambda \boldsymbol{I}\nabla \cdot \boldsymbol{u} + \mu\left[\nabla\boldsymbol{u} + (\nabla\boldsymbol{u})^{\mathrm{T}}\right],$$

or, in Cartesian components,

$$(3.7) \qquad E_{ijkl}\frac{\partial u_k}{\partial x_l} = \lambda\delta_{ij}\frac{\partial u_k}{\partial x_k} + \mu\left[\frac{\partial u_i}{\partial x_j} + \frac{\partial u_j}{\partial x_i}\right],$$

where δ_{ij} are the components of the identity matrix and λ, μ the constant Lamé coefficients of the material. $\quad \square$

Substituting Hooke's law (3.3) into the balance equations (3.1), we arrive at the boundary-value problem

$$
(3.8) \qquad
\begin{aligned}
-\nabla \cdot (\boldsymbol{E}\nabla\boldsymbol{u}) &= \boldsymbol{0} \quad \text{in } \Omega, \\
\boldsymbol{u} &= \boldsymbol{0} \quad \text{on } \Gamma_c, \\
\boldsymbol{n} \cdot (\boldsymbol{E}\nabla\boldsymbol{u}) &= \boldsymbol{0} \quad \text{on } \partial\omega, \\
\boldsymbol{n} \cdot (\boldsymbol{E}\nabla\boldsymbol{u}) &= \boldsymbol{t} \quad \text{on } \Gamma_t.
\end{aligned}
$$

4. The standard variational formulation. Weak solutions to problem (3.8) are defined using the following standard variational formulation:

find $\boldsymbol{u} \in \boldsymbol{V}$ such that

$$(4.1) \qquad \int_\Omega \nabla\boldsymbol{v} \cdot \boldsymbol{E}\nabla\boldsymbol{u} = \int_{\Gamma_t} \boldsymbol{v} \cdot \boldsymbol{t} \qquad \forall \boldsymbol{v} \in \boldsymbol{V},$$

where

$$(4.2) \qquad \boldsymbol{V} = \left\{\, \boldsymbol{v} \in \boldsymbol{H}^1(\Omega) \mid \gamma_{\Gamma_c}\boldsymbol{v} = \boldsymbol{0} \,\right\},$$

and where γ_{Γ_c} denotes the trace operator from $\boldsymbol{H}^1(\Omega)$ to $\boldsymbol{H}^{1/2}(\Gamma_c)$.

The well-posedness of problem (4.1) follows from the Lax–Milgram theorem [6, Thm. 2.5] due to the following standard properties.

---

[3]In components: $\alpha\tau_{ij}\tau_{ij} \leq \tau_{ij}E_{ijkl}\tau_{kl}$ for each τ_{ij} such that $\tau_{ij} = \tau_{ji}$.

(i) There is a $C_1 > 0$, depending on Ω and Γ_c, such that

$$(4.3) \qquad C_1 \|\boldsymbol{v}\|_{1,\Omega}^2 \leq \int_\Omega \nabla \boldsymbol{v} \cdot \boldsymbol{E} \nabla \boldsymbol{v} \quad \forall \boldsymbol{v} \in \boldsymbol{V}.$$

(ii) There is a constant C_2 such that

$$(4.4) \qquad \left| \int_\Omega \nabla \boldsymbol{v} \cdot \boldsymbol{E} \nabla \boldsymbol{u} \right| \leq C_2 |\boldsymbol{v}|_{1,\Omega} |\boldsymbol{u}|_{1,\Omega}$$
$$\leq C_2 \|\boldsymbol{v}\|_{1,\Omega} \|\boldsymbol{u}\|_{1,\Omega} \quad \forall \boldsymbol{u}, \boldsymbol{v} \in \boldsymbol{V}.$$

(iii) There is a constant C_3 such that

$$(4.5) \qquad \left| \int_{\Gamma_t} \boldsymbol{v} \cdot \boldsymbol{t} \right| \leq C_3 \|\boldsymbol{v}\|_{1,\Omega} \qquad \forall \boldsymbol{v} \in \boldsymbol{V}.$$

The coercivity property (i) follows from positivity assumption (3.5) together with Korn's 2nd inequality [6, Thm. 3.3]; assumption (3.2) is necessary for the latter to hold. The boundedness property (ii) is a consequence of the boundedness of the components of the elasticity tensor. The boundedness (iii) of the right-side linear form follows from boundedness of the trace operator on Γ_t. The value of constant C_3 depends on the surface traction $\boldsymbol{t}$, which we assume to be a given function in $\boldsymbol{L}^2(\Gamma_t)^d$ (although more general surface tractions in the direction of the discussion in section 7 could also have been specified).

5. The weak material approximation. Using the "material indicator" function

$$(5.1) \qquad \rho = \begin{cases} 1 & \text{in } \Omega, \\ 0 & \text{in } \omega, \end{cases}$$

variational form (4.1) can be written as a problem on the larger ground structure $\hat{\Omega}$:

$$(5.2) \qquad \begin{aligned} &\text{find } \boldsymbol{u} \in \hat{\boldsymbol{V}} \text{ such that} \\ &\int_{\hat{\Omega}} \rho \nabla \boldsymbol{v} \cdot \boldsymbol{E} \nabla \boldsymbol{u} = \int_{\Gamma_t} \boldsymbol{v} \cdot \boldsymbol{t} \qquad \forall \boldsymbol{v} \in \hat{\boldsymbol{V}}, \end{aligned}$$

where

$$(5.3) \qquad \hat{\boldsymbol{V}} = \left\{ \boldsymbol{v} \in \boldsymbol{H}^1(\hat{\Omega}) \mid \gamma_{\Gamma_c} \boldsymbol{v} = \boldsymbol{0} \right\},$$

and where here γ_{Γ_c} denotes the trace operator from $\boldsymbol{H}^1(\hat{\Omega})$ to $\boldsymbol{H}^{1/2}(\Gamma_c)$.

Formulation (5.2) is a "fictitious-domain" (or "domain embedding") formulation; that is, the problem is defined on the fixed domain $\hat{\Omega}$, and the presence of holes in the structure are represented by a vanishing material indicator ρ. In the discrete case, this formulation typically leads to a voxel- or pixel-based representation of the geometry, where each finite element is marked either as an element of material ($\rho = 1$) or an element of void ($\rho = 0$). In the material distribution approach to topology optimization, the material indicator function may be used as a design variable. For more details about the many issues that appear when using ρ in the context of topology optimization, we refer to the book by Bendsøe and Sigmund [4].

Unfortunately, the material indicator in equation (5.2) leaves the solution $\boldsymbol{u}$ undefined inside the hole. A cure for this problem, which is routinely applied when performing topology optimization [4, sect. 1.2.1], is to let $\rho \in \{\epsilon, 1\}$, with $0 < \epsilon \ll 1$.[4] Parameter ρ can be interpreted as a relative density, which means that the hole region is approximated with a region filled with a very weak material. In the two-dimensional case of plane stress, parameter ρ can also be interpreted as the relative thickness of a material plate; that is, the hole is approximated with a vanishingly thin sheet of material. Thus, using the weak material fictitious domain method, variational problem (4.1) is approximated by the following problem:

$$\text{(5.4)} \qquad \begin{aligned} &\text{find } \hat{\boldsymbol{u}}^\epsilon \in \hat{\boldsymbol{V}} \text{ such that} \\ &\int_\Omega \nabla \hat{\boldsymbol{v}}^\epsilon \cdot \boldsymbol{E} \nabla \hat{\boldsymbol{u}}^\epsilon + \epsilon \int_\omega \nabla \hat{\boldsymbol{v}}^\epsilon \cdot \boldsymbol{E} \nabla \hat{\boldsymbol{u}}^\epsilon = \int_{\Gamma_t} \hat{\boldsymbol{v}}^\epsilon \cdot \boldsymbol{t} \qquad \forall \hat{\boldsymbol{v}}^\epsilon \in \hat{\boldsymbol{V}}. \end{aligned}$$

(Note that we assumed that the elasticity tensor $\boldsymbol{E}$ is well defined and satisfies properties (3.5) also inside ω.) Using definitions

$$\text{(5.5a)} \qquad a_\alpha(\hat{\boldsymbol{v}}, \hat{\boldsymbol{u}}) = \int_\Omega \nabla \hat{\boldsymbol{v}} \cdot \boldsymbol{E} \nabla \hat{\boldsymbol{u}} + \alpha \int_\omega \nabla \hat{\boldsymbol{v}} \cdot \boldsymbol{E} \nabla \hat{\boldsymbol{u}},$$

$$\text{(5.5b)} \qquad l(\hat{\boldsymbol{v}}) = \int_{\Gamma_t} \hat{\boldsymbol{v}} \cdot \boldsymbol{t},$$

we may compactly write problem (5.4) as follows:

$$\text{(5.6)} \qquad \begin{aligned} &\text{find } \hat{\boldsymbol{u}}^\epsilon \in \hat{\boldsymbol{V}} \text{ such that} \\ &a_\epsilon(\hat{\boldsymbol{v}}^\epsilon, \hat{\boldsymbol{u}}^\epsilon) = l(\hat{\boldsymbol{v}}^\epsilon) \qquad \forall \hat{\boldsymbol{v}}^\epsilon \in \hat{\boldsymbol{V}}. \end{aligned}$$

The well-posedness of problem (5.6) is shown analogously as for problem (4.1). Boundedness of a_ϵ follows from boundedness of the elasticity tensor on $\hat{\Omega}$ and the Cauchy–Schwarz inequality; thus, there is a constant C such that

$$\text{(5.7)} \qquad |a_\epsilon(\hat{\boldsymbol{v}}, \hat{\boldsymbol{u}})| \le C \left(\|\hat{\boldsymbol{v}}\|_{1,\Omega} \|\hat{\boldsymbol{u}}\|_{1,\Omega} + \epsilon \|\hat{\boldsymbol{v}}\|_{1,\omega} \|\hat{\boldsymbol{u}}\|_{1,\omega} \right) \qquad \forall \hat{\boldsymbol{v}}, \hat{\boldsymbol{u}} \in \hat{\boldsymbol{V}}.$$

We will also need the following coercivity estimate.

LEMMA 5.1. *There is a $C > 0$ such that, for each $\epsilon \in [0, 1/2]$, it holds that*

$$\text{(5.8)} \qquad C \left(\|\hat{\boldsymbol{v}}\|_{1,\Omega}^2 + \epsilon \|\hat{\boldsymbol{v}}\|_{1,\omega}^2 \right) \le a_\epsilon(\hat{\boldsymbol{v}}, \hat{\boldsymbol{v}}) \qquad \forall \hat{\boldsymbol{v}} \in \hat{\boldsymbol{V}}.$$

Proof. First note that the elasticity bilinear form is coercive on $H^1(\Omega)$ as well as on $H^1(\hat{\Omega})$; that is, there are constants $C_\Omega, C_{\hat{\Omega}} > 0$ such that

$$\text{(5.9)} \qquad \begin{aligned} C_\Omega \|\boldsymbol{v}\|_{1,\Omega}^2 &\le \int_\Omega \nabla \boldsymbol{v} \cdot \boldsymbol{E} \nabla \boldsymbol{v} \qquad \forall \boldsymbol{v} \in \boldsymbol{V}, \\ C_{\hat{\Omega}} \|\hat{\boldsymbol{v}}\|_{1,\hat{\Omega}}^2 &\le \int_{\hat{\Omega}} \nabla \hat{\boldsymbol{v}} \cdot \boldsymbol{E} \nabla \hat{\boldsymbol{v}} \qquad \forall \hat{\boldsymbol{v}} \in \hat{\boldsymbol{V}}. \end{aligned}$$

---

[4]Moreover, to enable gradient-based optimization algorithms, the discrete feasible set $\{\epsilon, 1\}$ is commonly relaxed to $[\epsilon, 1]$, and a penalty is introduced that forces either $\rho \approx \epsilon$ or $\rho \approx 1$ [4, sect. 1.1.2].

For each $\hat{\boldsymbol{v}} \in \hat{\boldsymbol{V}}$ and for $\epsilon \in [0, 1/2]$, it holds that

$$
\begin{aligned}
a_\epsilon(\hat{\boldsymbol{v}}, \hat{\boldsymbol{v}}) &= \int_\Omega \nabla \boldsymbol{v} \cdot \boldsymbol{E} \nabla \boldsymbol{v} + \epsilon \int_\omega \nabla \boldsymbol{v} \cdot \boldsymbol{E} \nabla \boldsymbol{v} \\
&\geq \frac{1}{2} \int_\Omega \nabla \boldsymbol{v} \cdot \boldsymbol{E} \nabla \boldsymbol{v} + \epsilon \int_{\hat{\Omega}} \nabla \boldsymbol{v} \cdot \boldsymbol{E} \nabla \boldsymbol{v},
\end{aligned}
$$

(5.10)

$$
\begin{aligned}
[\text{ineq. (5.9)}] &\geq \frac{C_\Omega}{2} \|\hat{\boldsymbol{v}}\|_{1,\Omega}^2 + \epsilon\, C_{\hat{\Omega}} \|\hat{\boldsymbol{v}}\|_{1,\hat{\Omega}}^2 \\
&\geq \min\left(\frac{C_\Omega}{2}, C_{\hat{\Omega}}\right) \left(\|\hat{\boldsymbol{v}}\|_{1,\Omega}^2 + \epsilon \|\hat{\boldsymbol{v}}\|_{1,\omega}^2\right). \qquad \square
\end{aligned}
$$

Lemma 5.1 implies coercivity in $\boldsymbol{H}^1(\hat{\Omega})$ for all functions in $\hat{\boldsymbol{V}}$ as long as $\epsilon > 0$. Very small values of ϵ can be a source of ill-conditioning, as discussed in section 9. Lemma 5.1 also implies that for $\epsilon \in (0, 1/2]$, the bilinear form (5.5a) defines an inner product on $\boldsymbol{X} \times \boldsymbol{X}$, where $\boldsymbol{X}$ is any closed subspace of $\hat{\boldsymbol{V}}$, and we use the notation

(5.11)
$$
\|\hat{\boldsymbol{v}}\|_{a_\epsilon} = a_\epsilon(\hat{\boldsymbol{v}}, \hat{\boldsymbol{v}})^{1/2}
$$

for the corresponding induced norm. The Cauchy–Schwarz inequality for a_ϵ on $\boldsymbol{X} \times \boldsymbol{X}$ yields the characterization

(5.12)
$$
\|\hat{\boldsymbol{v}}\|_{a_\epsilon} = \sup_{\substack{\boldsymbol{w} \in \boldsymbol{X} \\ \boldsymbol{w} \neq \boldsymbol{0}}} \frac{a_\epsilon(\boldsymbol{w}, \hat{\boldsymbol{v}})}{\|\boldsymbol{w}\|_{a_\epsilon}},
$$

which will be used in the error analysis below.

For a finite-element discretization of problem (5.6), we introduce a family of triangulations $\{\hat{\mathcal{T}}^h\}_{h \in (0,1]}$ of $\hat{\Omega}$, such that $\operatorname{diam} K$, the diameter of any element $K \in \hat{\mathcal{T}}^h$ (triangles for $d = 2$, tetrahedra for $d = 3$), is bounded by $h \operatorname{diam} \Omega$. We assume that the family is nondegenerate; that is, for each element in a mesh, the quotient between the diameter of the largest ball inscribed in the element and the element diameter is uniformly, with respect to $h \in (0, 1]$, bounded away from zero [7, Def. 4.4.13]. In order to avoid complications associated with domain approximations, we assume that $\hat{\Omega}$ is polyhedral and Lipschitz and that the hole boundaries agrees with the element boundaries; that is, for each $K \in \hat{\mathcal{T}}^h$, it holds that either $K \subset \Omega$ or $K \subset \omega$. The results we achieve under this assumption, such as the relation to the elastic extension, as detailed below, constitute a basis for a treatment of the general nonaligned mesh case, which we refrain from treating in order to keep the presentation at a reasonable length. Associated with triangulation $\hat{\mathcal{T}}^h$, we introduce a finite-element subspaces $\hat{V}_h \subset H^1(\hat{\Omega})$ for each component of the vector-valued functions in $\hat{\boldsymbol{V}}_h$. We assume Lagrangian elements (of arbitrary order p), which means that we may expand each function $\hat{v}_h \in \hat{V}_h$ in the standard Lagrangian basis,

(5.13)
$$
\hat{v}_h(\boldsymbol{x}) = \sum_{i \in \mathcal{N}_h(\hat{\Omega})} v_i \phi_i(\boldsymbol{x}),
$$

where $v_i = \hat{v}_h(\boldsymbol{x}_i)$, the value of $\hat{v}_h$ at nodal point $\boldsymbol{x}_i \in \hat{\Omega}$; ϕ_i is the corresponding Lagrangian basis function; and $\mathcal{N}_h(\sigma)$ denotes the set of nodal indices occurring in point set $\sigma \subset \hat{\Omega}$. Functions in $\hat{\boldsymbol{V}}_h$ satisfy the following standard approximation properties [7, Thm. 4.4.20]: for σ being either ω or Ω, there is a constant C such that, for $0 \leq s \leq p$,

(5.14)
$$
\|\boldsymbol{v} - \Pi_p^h \boldsymbol{v}\|_{1,\sigma} \leq C h^s \|\boldsymbol{v}\|_{s+1,\sigma},
$$

where Π_p^h is the standard nodal interpolant into $\hat{\boldsymbol{V}}_h$.

A finite-element discretization of problem (5.6) may thus be formulated as follows:

$$(5.15) \qquad \begin{aligned} &\text{find } \hat{\boldsymbol{u}}_h^\epsilon \in \hat{\boldsymbol{V}}_h \text{ such that} \\ &a_\epsilon(\hat{\boldsymbol{v}}_h, \hat{\boldsymbol{u}}_h^\epsilon) = l(\hat{\boldsymbol{v}}_h) \qquad \forall \hat{\boldsymbol{v}}_h \in \hat{\boldsymbol{V}}_h. \end{aligned}$$

The question for the rest of this article is to quantify the error $\boldsymbol{u} - \hat{\boldsymbol{u}}_h^\epsilon|_\Omega$, the conditioning of the linear system associated with problem (5.15), and strategies to precondition the corresponding matrix.

Numerical experience indicates that the artificial solution $\boldsymbol{u}_h^\epsilon|_\omega$ is well defined as $\epsilon \to 0$. We will show that $\boldsymbol{u}_h^\epsilon|_\omega$ in fact approximates a relevant quantity, namely, the continuous elastic extension of $\boldsymbol{u}$ into ω, a quantity that also will appear in the estimate of $\boldsymbol{u} - \hat{\boldsymbol{u}}_h^\epsilon|_\Omega$.

6. The continuous elastic extension. Given the solution $\boldsymbol{u}$ to problem (3.8), we define the *continuous elastic extension of $\boldsymbol{u}$ into ω* as the solution $\boldsymbol{u}^\omega$ to the pure displacement problem

$$(6.1) \qquad \begin{aligned} -\nabla \cdot (\boldsymbol{E}\nabla\boldsymbol{u}^\omega) &= \boldsymbol{0} \quad \text{in } \omega, \\ \boldsymbol{u}^\omega &= \boldsymbol{u} \quad \text{on } \partial\omega, \end{aligned}$$

or, in variational form,

$$(6.2) \qquad \begin{aligned} &\text{find } \boldsymbol{u}^\omega \in \boldsymbol{H}^1(\omega) \text{ such that } \boldsymbol{u}^\omega = \boldsymbol{u} \text{ on } \partial\omega \text{ and} \\ &\int_\omega \nabla\boldsymbol{v}^\omega \cdot \boldsymbol{E}\nabla\boldsymbol{u}^\omega = \boldsymbol{0} \quad \forall \boldsymbol{v}^\omega \in \boldsymbol{H}_0^1(\omega). \end{aligned}$$

Well-posedness of problem (6.2) follows, again, from the Lax–Milgram lemma, along the same lines as discussed in section 4, together with the trace theorem on $\partial\omega$ from ω and Ω, respectively.

Now we may define a compound object $\hat{\boldsymbol{u}} \in \hat{\boldsymbol{V}}$ as

$$(6.3) \qquad \hat{\boldsymbol{u}} = \begin{cases} \boldsymbol{u} & \text{in } \Omega, \\ \boldsymbol{u}^\omega & \text{in } \omega. \end{cases}$$

However, instead of defining $\hat{\boldsymbol{u}}$ as in expression (6.3)—through consecutive solutions of variational problems (4.1) and (6.2)—it will turn out to be more illuminating in this context to introduce a unified, single variational form for $\hat{\boldsymbol{u}}$. For this, let $\hat{\boldsymbol{u}}$ be defined as above, choose $\alpha > 0$ arbitrarily, and sum equations (4.1) and (6.2) to find that $\hat{\boldsymbol{u}} \in \hat{\boldsymbol{V}}$ satisfies

$$(6.4) \qquad \int_\Omega \nabla\boldsymbol{v} \cdot \boldsymbol{E}\nabla\hat{\boldsymbol{u}} + \alpha \int_\omega \nabla\boldsymbol{w}^\omega \cdot \boldsymbol{E}\nabla\hat{\boldsymbol{u}} = \int_{\Gamma_t} \boldsymbol{v} \cdot \boldsymbol{t}$$

for each $\boldsymbol{v} \in \boldsymbol{V}$ and $\boldsymbol{w}^\omega \in \boldsymbol{H}_0^1(\omega)$. Collecting the test functions in expression (6.4) into a space of functions on $\hat{\Omega}$,

$$(6.5) \qquad \hat{\boldsymbol{W}} = \left\{ \hat{\boldsymbol{v}} \in \boldsymbol{L}^2(\hat{\Omega}) \mid \hat{\boldsymbol{v}}|_\Omega \in \boldsymbol{V}, \, \hat{\boldsymbol{v}}|_\omega \in \boldsymbol{H}_0^1(\omega) \right\},$$

and utilizing previous definitions (5.5), we arrive at the following unified variational problem:

$$(6.6) \qquad \begin{aligned} &\text{find } \hat{\boldsymbol{u}} \in \hat{\boldsymbol{V}} \text{ such that} \\ &a_\alpha(\hat{\boldsymbol{v}}, \hat{\boldsymbol{u}}) = l(\hat{\boldsymbol{v}}) \qquad \forall \hat{\boldsymbol{v}} \in \hat{\boldsymbol{W}}. \end{aligned}$$

Note that the continuity of $\hat{\boldsymbol{u}}$ at the hole boundaries, explicitly enforced in the formulation (6.2), is implicit in variational formulation (6.6) through to the definition of the trial space $\hat{\boldsymbol{V}}$. We have thus arrived at the following equivalence property.

THEOREM 6.1. $\hat{\boldsymbol{u}} \in \boldsymbol{V}$ *solves problems* (4.1) *and* (6.2) *if and only if* $\hat{\boldsymbol{u}}$ *solves problem* (6.6).

Proof. The derivation above shows that if $\hat{\boldsymbol{u}}$ solves problems (4.1) and (6.2) then $\hat{\boldsymbol{u}}$ satisfies variational expression (6.6). For the reverse implication, assume that $\hat{\boldsymbol{u}} \in \hat{\boldsymbol{V}}$ solves problem (6.6). Selecting in variational expression (6.6) test functions $\hat{\boldsymbol{v}} \in \hat{\boldsymbol{W}}$ with support first solely in Ω and then solely in ω, we recover variational expressions (4.1) and (6.2). Since $\hat{\boldsymbol{u}} \in \boldsymbol{H}^1(\hat{\Omega})$, the trace theorem for $\boldsymbol{H}^1(\hat{\Omega})$ functions on Lipschitz domains [21, Thm. 8.7] yields continuity for $\hat{\boldsymbol{u}}$ at $\partial\omega$. We thus find that $\hat{\boldsymbol{u}}$ satisfies the essential boundary condition in problem (6.2). $\quad\square$

Note that problem (6.6) involves the same bilinear form as in the weak material problem (5.15), which means that the weak material problem (5.15) can be interpreted as a nonconforming approximation of problem (6.6); it is nonconforming since the space of discrete test functions $\hat{\boldsymbol{V}}_h$ in problem (5.15) is not a subspace of $\hat{\boldsymbol{W}}$, the space of test function in problem (6.6). Nevertheless, we will show in Theorem 8.3 below that the solution $\hat{\boldsymbol{u}}_h^\epsilon$ to problem (5.15) continuously approaches the solution of the extended problem (6.6) as $h, \epsilon \to 0$.

Moreover, Theorem 9.3 below shows that an appropriately preconditioned version of the weak material finite-element problem (5.15) admits the limit value $\epsilon = 0$ without generating a singular stiffness matrix, and that this preconditioned version with $\epsilon = 0$ yields a finite-element approximation of the extended problem (6.6). This limit finite-element approximation involves a discrete subspace of $\hat{\boldsymbol{W}}$ that can be constructed by projections of the basis functions $\phi_i \in \hat{V}_h^h$. We define the space $\hat{W}_h$ as the linear span over all $i \in \mathcal{N}_h(\hat{\Omega})$ of the basis functions $\tilde{\phi}_i$, given by

$$(6.7) \qquad \tilde{\phi}_i = \begin{cases} \chi_\Omega \, \phi_i & \text{for } i \in \mathcal{N}_h(\Gamma), \\ \phi_i & \text{otherwise,} \end{cases}$$

where χ_Ω is the characteristic functions on Ω. We then define $\hat{\boldsymbol{W}}_h = \hat{W}_h^d \subset \hat{\boldsymbol{W}}$ and arrive at the following finite-element approximation of the extended problem (6.6):

$$(6.8) \qquad \begin{aligned} &\text{find } \hat{\boldsymbol{u}}_h \in \hat{\boldsymbol{V}}_h \text{ such that} \\ &a_\alpha(\hat{\boldsymbol{v}}_h, \hat{\boldsymbol{u}}_h) = l(\hat{\boldsymbol{v}}_h) \qquad \forall \hat{\boldsymbol{v}}_h \in \hat{\boldsymbol{W}}_h. \end{aligned}$$

7. Surface tractions on $\partial\omega$. The extended displacement field $\hat{\boldsymbol{u}}$, defined either through expression (6.3) or, equivalently, as the solution to problem (6.6), is continuous at $\partial\omega$. However, the corresponding surface traction will in general exhibit a jump discontinuity at $\partial\omega$: the surface traction vanishes when approaching $\partial\omega$ from the inside of Ω, due to the boundary condition of problem (3.8), but will generally be nonzero when approaching from the inside of ω, due to the required displacement condition on $\partial\omega$ in problem (6.1). We will derive a variational expression for the surface traction from the inside, an expression that naturally will appear in the error analysis in section 8.

First assume that the boundary displacement data is smooth enough so that the solution to problem (6.2) satisfies $\boldsymbol{u}^\omega \in \boldsymbol{H}^2(\omega)$. Boundary-value problem (6.1) is then satisfied in a strong sense. Let $\boldsymbol{n}$ denote the normal vector field on $\partial\omega$, outward-directed with respect to ω. The d-vector defined through

$$(7.1) \qquad \boldsymbol{\lambda}(\boldsymbol{u}^\omega) = \boldsymbol{\sigma}(\boldsymbol{u}^\omega)\boldsymbol{n} = \boldsymbol{n} \cdot \boldsymbol{E}\nabla\boldsymbol{u}^\omega$$

is the surface traction on $\partial\omega$ when approaching the surface from inside of ω. Each component of $\boldsymbol{\lambda}(\boldsymbol{u}^\omega)$ will be an $L^2(\partial\omega)$ function due to the requested regularity of $\boldsymbol{u}^\omega$ and $\partial\omega$. Taking the dot product of each side of expression (7.1) with an arbitrary function $\boldsymbol{\Psi} \in \boldsymbol{H}^1(\omega)$ and integrating by parts yields

$$(7.2) \quad \int_{\partial\omega} \boldsymbol{\Psi} \cdot \boldsymbol{\lambda}(\boldsymbol{u}^\omega) = \int_{\partial\omega} \boldsymbol{\Psi} \cdot \boldsymbol{\sigma}(\boldsymbol{u}^\omega)\boldsymbol{n} = \int_\omega \nabla\boldsymbol{\Psi} \cdot \boldsymbol{\sigma}(\boldsymbol{u}^\omega) + \int_\omega \boldsymbol{\Psi} \cdot \left[\nabla \cdot \boldsymbol{\sigma}(\boldsymbol{u}^\omega)\right]$$
$$= \int_\omega \nabla\boldsymbol{\Psi} \cdot \boldsymbol{\sigma}(\boldsymbol{u}^\omega) = \int_\omega \nabla\boldsymbol{\Psi} \cdot \boldsymbol{E}\nabla\boldsymbol{u}^\omega,$$

where the second term in the expression after the second equality vanishes due to equation (6.1). Thus, if $\boldsymbol{u}^\omega \in \boldsymbol{H}^2(\omega)$ solves equation (6.2), then the surface traction vector $\boldsymbol{\lambda}(\boldsymbol{u}^\omega)$ satisfies

$$(7.3) \quad \int_{\partial\omega} \boldsymbol{\lambda}(\boldsymbol{u}^\omega) \cdot \boldsymbol{\Psi} = \int_\omega \nabla\boldsymbol{\Psi} \cdot \boldsymbol{E}\nabla\boldsymbol{u}^\omega$$

for each $\boldsymbol{\Psi} \in \boldsymbol{H}^1(\omega)$. The above derivation of variational expression (7.3) required "full elliptic regularity," that is, that $\boldsymbol{u}^\omega \in \boldsymbol{H}^2(\omega)$. However, the right side of expression (7.3) is well defined for all weak solutions, also if it would merely hold that $\boldsymbol{u}^\omega \in \boldsymbol{H}^1(\omega)$. As we will see, this fact allows us to define surface tractions as a linear functional on the trace space $\boldsymbol{H}^{1/2}(\partial\omega)$ for each weak solution $\boldsymbol{u}^\omega \in \boldsymbol{H}^1(\omega)$. To do so, we start by defining a bounded linear functional associated with the right side of expression (7.3).

LEMMA 7.1. *For each $\boldsymbol{u} \in \boldsymbol{H}^1(\omega)$, the mapping $\boldsymbol{\lambda}(\boldsymbol{u}) : \boldsymbol{H}^{1/2}(\partial\omega) \to \mathbb{R}$, defined by its action on $\boldsymbol{g} \in \boldsymbol{H}^{1/2}(\partial\omega)$ through*

$$(7.4) \quad \langle\boldsymbol{\lambda}(\boldsymbol{u}), \boldsymbol{g}\rangle_{1/2,\partial\omega} = \int_\omega \nabla\mathcal{X}\boldsymbol{g} \cdot \boldsymbol{E}\nabla\boldsymbol{u},$$

where $\mathcal{X} : \boldsymbol{H}^{1/2}(\partial\omega) \to \boldsymbol{H}^1(\omega)$ is the minimum-norm extension operator (2.4), is a bounded linear functional on $\boldsymbol{H}^{1/2}(\partial\omega)$.

Proof. The linearity is immediate. Let $\boldsymbol{g} \in \boldsymbol{H}^{1/2}(\partial\omega)$ be given. The boundedness then follows from

$$(7.5) \quad \left|\langle\boldsymbol{\lambda}(\boldsymbol{u}), \boldsymbol{g}\rangle_{1/2,\partial\omega}\right| = \left|\int_\omega \nabla\mathcal{X}\boldsymbol{g} \cdot \boldsymbol{E}\nabla\boldsymbol{u}\right| \leq C_1\|\mathcal{X}\boldsymbol{g}\|_{1,\omega}\|\boldsymbol{u}\|_{1,\omega}$$
$$\leq C_1 C_2\|\boldsymbol{g}\|_{1/2,\partial\omega}\|\boldsymbol{u}\|_{1,\omega} \leq C_1 C_2 C_{\boldsymbol{u}}\|\boldsymbol{g}\|_{1/2,\partial\omega},$$

where the first inequality follows from the boundedness property (4.4), the second from property (2.4), and where $C_{\boldsymbol{u}} = \|\boldsymbol{u}\|_{1,\omega}$. $\quad\square$

Using Lemma 7.1, we may introduce the weak surface traction as an element in $\boldsymbol{H}^{-1/2}(\partial\omega)$.

DEFINITION 7.2. *The* weak surface traction *on $\partial\omega$ associated with a solution $\boldsymbol{u}^\omega$ to variational problem (6.2) is the linear functional $\lambda(\boldsymbol{u}^\omega)$ defined in expression (7.4).*

The following lemma is a consequence of the definition of the weak surface traction.

LEMMA 7.3. *The weak surface traction $\boldsymbol{\lambda}(\boldsymbol{u}^\omega)$ associated with the solution $\boldsymbol{u}^\omega \in \boldsymbol{H}^1(\omega)$ of problem (6.2) satisfies*

$$(7.6) \quad \langle\boldsymbol{\lambda}(\boldsymbol{u}^\omega), \gamma\boldsymbol{\Psi}\rangle_{1/2,\partial\omega} = \int_\omega \nabla\boldsymbol{\Psi} \cdot \boldsymbol{E}\nabla\boldsymbol{u}^\omega \qquad \forall\boldsymbol{\Psi} \in \boldsymbol{H}^1(\omega),$$

where γ is the trace map from $\boldsymbol{H}^1(\omega)$ to $\boldsymbol{H}^{1/2}(\omega)$.

Proof. Let $\boldsymbol{\Psi} \in \boldsymbol{H}^1(\omega)$ be given arbitrarily, let $\gamma : \boldsymbol{H}^1(\omega) \to \boldsymbol{H}^{1/2}(\partial\omega)$ be the trace map, and let $\mathcal{X} : \boldsymbol{H}^{1/2}(\partial\omega) \to \boldsymbol{H}^1(\omega)$ be the minimum-norm extension. We write

$$(7.7) \qquad \boldsymbol{\Psi} = \mathcal{X}\gamma\boldsymbol{\Psi} + \underbrace{\boldsymbol{\Psi} - \mathcal{X}\gamma\boldsymbol{\Psi}}_{\in \boldsymbol{H}_0^1(\omega)},$$

which yields that

$$
\begin{aligned}
(7.8) \qquad \int_\omega \nabla\boldsymbol{\Psi} \cdot \boldsymbol{E}\nabla\boldsymbol{u}^\omega &= \int_\omega \nabla\mathcal{X}\gamma\boldsymbol{\Psi} \cdot \boldsymbol{E}\nabla\boldsymbol{u}^\omega + \int_\omega \nabla(\boldsymbol{\Psi} - \mathcal{X}\gamma\boldsymbol{\Psi}) \cdot \boldsymbol{E}\nabla\boldsymbol{u}^\omega \\
&= \int_\omega \nabla\mathcal{X}\gamma\boldsymbol{\Psi} \cdot \boldsymbol{E}\nabla\boldsymbol{u}^\omega = \langle \boldsymbol{\lambda}(\boldsymbol{u}^\omega), \gamma\boldsymbol{\Psi} \rangle_{1/2,\partial\omega},
\end{aligned}
$$

where the second equality follows from equation (6.2) with $\boldsymbol{v} = \boldsymbol{\Psi} - \mathcal{X}\gamma\boldsymbol{\Psi}$ and the third equality from definition (7.4). □

Thus, to summarize, the surface traction on $\partial\omega$, generated by the continuous elastic extension inside the hole region ω, satisfies expression (7.6), and the linear functional has the integral representation (7.3) for elastic extensions that are smooth enough.

8. Error analysis. A useful tool in the error analysis will be a projector P_h on $\hat{V}_h$ that causes functions in $\hat{V}_h$ to vanish at each finite-element node that is located strictly interior in ω but otherwise leaves the function unchanged. For Lagrangian elements, the action of P_h is accomplished by restricting expansion (5.13) to the nonhole region $\overline{\Omega}$,

$$(8.1) \qquad P_h\hat{v}_h = \sum_{i\in\mathcal{N}_h(\overline{\Omega})} v_i\phi_i.$$

Figure 8.1 illustrates the action of P_h in the one-dimensional case when using linear elements. Figure 8.2 visualizes the support of the function $P_h\hat{v}_h$ in the two-dimensional setup of Figure 3.1. Note that the support extends into the first layer of triangles in the hole region ω. Operator P_h is constructed in order to fulfill properties

$$
\begin{aligned}
(8.2) \qquad (P_h\hat{v}_h)|_{\overline{\Omega}} &= \hat{v}_h|_{\overline{\Omega}}, \\
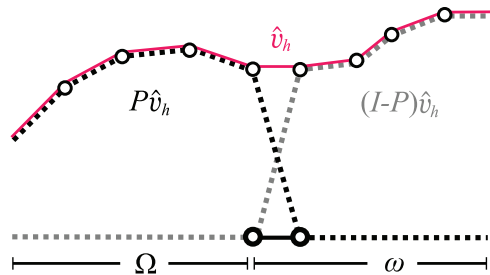(I - P_h)v_h|_\omega &\in H_0^1(\omega) \cap V_h|_\omega.
\end{aligned}
$$

FIG. 8.1. *The action of operator P_h for $d = 1$ when using linear Lagrangian elements: the original function $\hat{v}_h$ (thin solid line), the function $P_h\hat{v}_h$ (black dashed line), and $(I - P_h)\hat{v}_h$ (gray dashed line).*
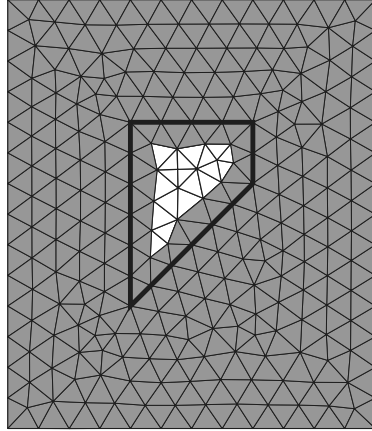
FIG. 8.2. *The gray region indicates the support of the function $P_h\hat{v}_h$ in the setup of Figure* 3.1 *when using linear Lagrangian elements.*

For $\boldsymbol{v}_h \in \boldsymbol{V}_h$, we define $\boldsymbol{P}_h\boldsymbol{v}_h$ by the action of P_h on each component of $\boldsymbol{v}_h$.

Problem (5.15) constitutes a nonconforming approximation of problem (6.6) since $\hat{\boldsymbol{V}}_h \not\subset \hat{\boldsymbol{W}}$, so the first step in the error analysis is to estimate the consistency error.

LEMMA 8.1. *The solutions $\hat{\boldsymbol{u}}$ and $\hat{\boldsymbol{u}}_h^\epsilon$ to equations* (6.6) *and* (5.15) *satisfy*

$$(8.3) \qquad a_\epsilon(\hat{\boldsymbol{v}}_h, \hat{\boldsymbol{u}} - \hat{\boldsymbol{u}}_h^\epsilon) = \epsilon\langle\boldsymbol{\lambda}(\boldsymbol{u}^\omega), \gamma_{\partial\omega}\boldsymbol{v}_h\rangle_{1/2,\partial\omega} \qquad \forall\hat{\boldsymbol{v}}_h \in \hat{\boldsymbol{V}}_h,$$

where $\boldsymbol{u}^\omega = \hat{\boldsymbol{u}}|_\omega$.

Proof. Given any $\hat{\boldsymbol{v}}_h \in \hat{\boldsymbol{V}}_h$, we may use properties (8.2) to construct a function $\hat{\boldsymbol{w}}_h \in \hat{\boldsymbol{W}}$ by

$$(8.4) \qquad \hat{\boldsymbol{w}}_h = \begin{cases} \hat{\boldsymbol{v}}_h|_\Omega & \text{in } \Omega, \\ (\boldsymbol{I} - \boldsymbol{P}_h)\hat{\boldsymbol{v}}_h|_\omega & \text{in } \omega. \end{cases}$$

We note that

$$(8.5) \qquad l(\hat{\boldsymbol{w}}_h) = l(\hat{\boldsymbol{v}}_h)$$

by definition (5.5b) and property (8.2).

The solution $\hat{\boldsymbol{u}}$ to equation (6.6) satisfies

$$
\begin{aligned}
a_\epsilon(\hat{\boldsymbol{v}}_h, \hat{\boldsymbol{u}}) &= \int_\Omega \nabla\hat{\boldsymbol{v}}_h \cdot \boldsymbol{E}\nabla\hat{\boldsymbol{u}} + \epsilon\int_\omega \nabla\big[\boldsymbol{P}_h\hat{\boldsymbol{v}}_h + (\boldsymbol{I} - \boldsymbol{P}_h)\hat{\boldsymbol{v}}_h\big] \cdot \boldsymbol{E}\nabla\hat{\boldsymbol{u}} \\
&= \int_\Omega \nabla\hat{\boldsymbol{v}}_h \cdot \boldsymbol{E}\nabla\hat{\boldsymbol{u}} + \epsilon\int_\omega \nabla(\boldsymbol{I} - \boldsymbol{P}_h)\hat{\boldsymbol{v}}_h \cdot \boldsymbol{E}\nabla\hat{\boldsymbol{u}} + \epsilon\int_\omega \nabla\boldsymbol{P}_h\hat{\boldsymbol{v}}_h \cdot \boldsymbol{E}\nabla\hat{\boldsymbol{u}} \\
(8.6) \qquad &= a_\epsilon(\hat{\boldsymbol{w}}_h, \hat{\boldsymbol{u}}) + \epsilon\int_\omega \nabla\boldsymbol{P}_h\hat{\boldsymbol{v}}_h \cdot \boldsymbol{E}\nabla\hat{\boldsymbol{u}} = l(\hat{\boldsymbol{v}}_h, \hat{\boldsymbol{u}}) + \epsilon\int_\omega \nabla\boldsymbol{P}_h\hat{\boldsymbol{v}}_h \cdot \boldsymbol{E}\nabla\boldsymbol{u}^\omega \\
&= l(\hat{\boldsymbol{v}}_h, \hat{\boldsymbol{u}}) + \epsilon\langle\boldsymbol{\lambda}(\boldsymbol{u}^\omega), \gamma_{\partial\omega}\boldsymbol{v}_h\rangle_{1/2,\partial\omega},
\end{aligned}
$$

where the third equality follows from definitions (5.5a) and (8.4), the fourth from equation (6.6) and from property (8.5), and the fifth from Lemma 7.3. Subtracting equation (5.15) from expression (8.6) yields the claim. $\quad\square$

Lemma 8.1 implies the following inconsistency bound.

LEMMA 8.2. *There is a constant C such that*

$$(8.7) \qquad \sup_{\substack{\boldsymbol{w} \in \hat{\boldsymbol{V}}_h \\ \boldsymbol{w} \neq \boldsymbol{0}}} \frac{a_\epsilon(\boldsymbol{w}, \hat{\boldsymbol{u}} - \hat{\boldsymbol{u}}_h^\epsilon)}{\|\boldsymbol{w}\|_{a_\epsilon}} \leq \epsilon C \|\boldsymbol{\lambda}(\boldsymbol{u}^\omega)\|_{-1/2,\partial\omega}.$$

Proof. Denote by $\tilde{\gamma}_{\partial\omega} : H^1(\Omega) \to H^{1/2}(\partial\omega)$ and $\gamma_{\partial\omega} : H^1(\omega) \to H^{1/2}(\partial\omega)$ the trace maps on $\partial\omega$ from Ω and ω, respectively. Note that for $\hat{w} \in H^1(\hat{\Omega})$, $\tilde{\gamma}_{\partial\omega}\hat{w}|_\Omega = \gamma_{\partial\omega}\hat{w}|_\omega$. Letting $\boldsymbol{0} \neq \hat{\boldsymbol{w}}_h \in \hat{\boldsymbol{V}}_h$ be given arbitrarily, it holds that

$$(8.8) \qquad \|\gamma_{\partial\omega}\hat{\boldsymbol{w}}_h\|_{1/2,\partial\omega} = \|\tilde{\gamma}_{\partial\omega}\hat{\boldsymbol{w}}_h\|_{1/2,\partial\omega} \leq C\|\hat{\boldsymbol{w}}_h\|_{1,\Omega} \leq C\|\hat{\boldsymbol{w}}_h\|_{a_\epsilon},$$

where C is the constant of trace inequality (2.6) applied on $\tilde{\gamma}_{\partial\omega}$, and where the last inequality follows from definitions (5.5a) and (5.11). Lemma 8.1, inequality (8.8), and definition (2.7) imply that

$$(8.9) \qquad \frac{a_\epsilon(\hat{\boldsymbol{w}}, \hat{\boldsymbol{u}} - \hat{\boldsymbol{u}}_h^\epsilon)}{\|\hat{\boldsymbol{w}}\|_{a_\epsilon}} \leq \epsilon C \frac{\langle \boldsymbol{\lambda}(\boldsymbol{u}^\omega), \gamma_{\partial\omega}\hat{\boldsymbol{w}}_h \rangle_{1/2,\partial\omega}}{\|\gamma_{\partial\omega}\hat{\boldsymbol{w}}_h\|_{1/2,\partial\omega}} \leq \epsilon C \|\boldsymbol{\lambda}(\boldsymbol{u}^\omega)\|_{-1/2,\partial\omega},$$

from which the conclusion follows. $\square$

We are now ready to estimate the error associated with finite-element solution when the weak-material approximation is employed. The maximal values of s and s' in estimate (8.10) are case dependent and depend on the regularity of $\boldsymbol{u}$ and $\boldsymbol{u}^\omega$, respectively.

THEOREM 8.3. *There is a constant $C > 0$ such that the solution $\hat{\boldsymbol{u}}_h^\epsilon$ of the weak-material approximation problem (5.4) satisfies, for $0 \leq s, s' \leq p$,*

$$(8.10) \qquad C\|\boldsymbol{u} - \hat{\boldsymbol{u}}_h^\epsilon\|_{1,\Omega} \leq h^s\|\boldsymbol{u}\|_{s+1,\Omega} + \epsilon^{1/2}h^{s'}\|\boldsymbol{u}^\omega\|_{s'+1,\Omega} + \epsilon \|\lambda(\boldsymbol{u}^\omega)\|_{-1/2,\partial\omega},$$

where $\boldsymbol{u}$ is the solution to problem (4.1), $\boldsymbol{u}^\omega$ is the continuous elastic extension of $\boldsymbol{u}$ into ω, defined in equation (6.2), and $\lambda(\boldsymbol{u}^\omega)$ is the surface traction on $\partial\omega$ according to Definition 7.2.

Proof. Let C_1 be the square root of the coercivity constant in Lemma 5.1, C_2 the constant of Lemma 8.2, and C_3 the constant of inequality (5.7). For each $\hat{\boldsymbol{v}}_h \in \hat{\boldsymbol{V}}_h$, it holds that

$$C_1\|\boldsymbol{u} - \hat{\boldsymbol{u}}_h^\epsilon\|_{1,\Omega} \leq C_1 \left[\|\boldsymbol{u} - \hat{\boldsymbol{u}}_h^\epsilon\|_{1,\Omega}^2 + \epsilon\|\boldsymbol{u}^\omega - \hat{\boldsymbol{u}}_h^\epsilon\|_{1,\omega}^2 \right]^{1/2}$$

$$[(5.8)] \; \leq \|\hat{\boldsymbol{u}} - \hat{\boldsymbol{u}}_h^\epsilon\|_{a_\epsilon} \leq \|\hat{\boldsymbol{u}} - \hat{\boldsymbol{v}}_h\|_{a_\epsilon} + \|\hat{\boldsymbol{v}}_h - \hat{\boldsymbol{u}}_h^\epsilon\|_{a_\epsilon}$$

$$[(5.12)] = \|\hat{\boldsymbol{u}} - \hat{\boldsymbol{v}}_h\|_{a_\epsilon} + \sup_{\substack{\boldsymbol{w} \in \hat{\boldsymbol{V}}_h \\ \boldsymbol{w} \neq \boldsymbol{0}}} \frac{a_\epsilon(\boldsymbol{w}, \hat{\boldsymbol{v}}_h - \hat{\boldsymbol{u}}_h^\epsilon)}{\|\boldsymbol{w}\|_{a_\epsilon}}$$

$$[\text{add \& subtr. } \hat{\boldsymbol{u}}] \leq \|\hat{\boldsymbol{u}} - \hat{\boldsymbol{v}}_h\|_{a_\epsilon} + \sup_{\substack{\boldsymbol{w} \in \hat{\boldsymbol{V}}_h \\ \boldsymbol{w} \neq \boldsymbol{0}}} \frac{a_\epsilon(\boldsymbol{w}, \hat{\boldsymbol{v}}_h - \hat{\boldsymbol{u}})}{\|\boldsymbol{w}\|_{a_\epsilon}} + \sup_{\substack{\boldsymbol{w} \in \hat{\boldsymbol{V}}_h \\ \boldsymbol{w} \neq \boldsymbol{0}}} \frac{a_\epsilon(\boldsymbol{w}, \hat{\boldsymbol{u}} - \hat{\boldsymbol{u}}_h^\epsilon)}{\|\boldsymbol{w}\|_{a_\epsilon}}$$

$$[(5.12), \text{Lemma 8.2}] \leq 2\|\hat{\boldsymbol{u}} - \hat{\boldsymbol{v}}_h\|_{a_\epsilon} + \epsilon C_2 \|\boldsymbol{\lambda}(\hat{\boldsymbol{u}})\|_{-1/2,\partial\omega}$$

$$[(5.7)] \leq 2C_3 \left[\|\hat{\boldsymbol{u}} - \hat{\boldsymbol{v}}_h\|_{1,\Omega}^2 + \epsilon\|\hat{\boldsymbol{u}} - \hat{\boldsymbol{v}}_h\|_{1,\omega}^2 \right]^{1/2} + \epsilon C_2 \|\boldsymbol{\lambda}(\hat{\boldsymbol{u}})\|_{-1/2,\partial\omega}$$

$$[\triangle\text{-ineq.}] \leq 2C_3 \left[\|\hat{\boldsymbol{u}} - \hat{\boldsymbol{v}}_h\|_{1,\Omega} + \epsilon^{1/2}\|\hat{\boldsymbol{u}} - \hat{\boldsymbol{v}}_h\|_{1,\omega} \right] + \epsilon C_2 \|\boldsymbol{\lambda}(\hat{\boldsymbol{u}})\|_{-1/2,\partial\omega}.$$

Now we choose $\hat{\boldsymbol{v}}_h|_\Omega$ and $\hat{\boldsymbol{v}}_h|_\omega$ as the nodal interpolant of $\hat{\boldsymbol{u}}|_\Omega = \boldsymbol{u}$ and $\hat{\boldsymbol{u}}|_\omega = \boldsymbol{u}^\omega$, respectively. (Note the interpolated functions coincide on $\partial\omega$ since the solution is

continuous on $\partial\omega$.) The conclusion, with $C = \min\{\, C_1/(2C_3), C_1/C_2 \,\}$, then follows by interpolation estimate (5.14). $\square$

The error bound (8.10) approaches in the limit $\epsilon \to 0$ the error bound for a finite-element approximation of the standard variational problem (4.1). Thus, the smaller the ϵ, the less the error will be from the weak material approximation. However, the condition number of the stiffness matrix will grow as ϵ is decreased, as quantified in the next section.

9. Conditioning of the linear system. Recall that each function v_h in the scalar finite-element space $\hat{V}^h$ can be expanded, as in expression (5.13), in the standard Lagrangian basis ϕ_i, $i = 1, \ldots, N$, where N is the number of nodes in $\hat{\Omega}$. We construct a vector basis of $\hat{\boldsymbol{V}}_h$ from the scalar basis ϕ_i through expression

$$(9.1) \qquad \boldsymbol{\phi}_{d(i-1)+k} = \phi_i \boldsymbol{e}_k \qquad i = 1, \ldots, N,\, k = 1, \ldots, d,$$

where $\boldsymbol{e}_k$ are unit Cartesian basis vectors in $\mathbb{R}^d$. Any function $\boldsymbol{v}_h \in \hat{\boldsymbol{V}}_h$ may then be expanded in the basis (9.1):

$$(9.2) \qquad \boldsymbol{v}_h = \sum_{i=1}^{dN} v_i \boldsymbol{\phi}_i.$$

Denote by $\mathbf{v} = (v_1, \ldots, v_{dN})^T$ the column vector (the dN-by-1 matrix) of the nodal values of $\boldsymbol{v}_h$ in expansion (9.2). We choose a numbering of the nodes so that $\mathbf{v}$ may be partitioned as

$$(9.3) \qquad \mathbf{v} = \begin{pmatrix} \mathbf{v}_\Omega \\ \mathbf{v}_\Gamma \\ \mathbf{v}_{\omega,} \end{pmatrix},$$

that is, into groups of nodal values located in Ω, Γ, and ω, respectively. Denote by N_Ω, N_Γ, and N_ω the lengths of column vectors $\mathbf{v}_\Omega$, $\mathbf{v}_\Gamma$, and $\mathbf{v}_\omega$, respectively.

Let $\mathbf{e}_i$, $i = 1, \ldots, dN$, denote the ith column of the dN-by-dN identity matrix. Finite-element problem (5.15) gives rise to a dN-by-dN stiffness matrix $\mathbf{A}_\epsilon$ defined by

$$(9.4) \qquad \mathbf{e}_i^T \mathbf{A}_\epsilon \mathbf{e}_j = a_\epsilon(\boldsymbol{\phi}_i, \boldsymbol{\phi}_j).$$

Thus, for each $\hat{\boldsymbol{v}}_h, \hat{\boldsymbol{u}}_h \in \hat{\boldsymbol{V}}_h$ and for column vectors $\mathbf{v}$, $\mathbf{u}$ that contain corresponding nodal values, it holds that

$$(9.5) \qquad \mathbf{v}^T \mathbf{A}_\epsilon \mathbf{u} = a_\epsilon(\hat{\boldsymbol{v}}_h, \hat{\boldsymbol{u}}_h).$$

We will estimate the spectral condition number $\kappa(\mathbf{A}_\epsilon)$, that is, the quotient of the largest and smallest eigenvalues of $\mathbf{A}_\epsilon$. Since the matrix is symmetric, these eigenvalues can be estimated through upper and lower bounds of the associated quadratic form $\mathbf{v}^T \mathbf{A}_\epsilon \mathbf{v}$ for unit-norm column vectors $\mathbf{v}$.

Such bounds require additional assumptions on the mesh. Here we make the standard assumption that the mesh family is quasi-uniform, that is, that $\max_{K \in \mathcal{T}^h} h/\rho_K$, where ρ_K is the largest ball contained in K, is uniformly bounded for $h \in (0, 1]$ [7, Def. 4.4.13].

For each mesh in a quasi-uniform family of meshes, there is an equivalence between the L^2 norm of finite-element functions and the two-norm of corresponding column

vectors containing nodal values. By applying this equivalence property, proven by Quarteroni and Valli [17, Prop. 6.3.1], to restrictions on $\overline{\Omega}$ and $\overline{\omega}$ of functions $\hat{\boldsymbol{v}}_h \in \hat{\boldsymbol{V}}_h$, it follows that there are C_l, $C_u > 0$ such that, for $h \in (0, 1]$,

$$
(9.6) \quad
\begin{aligned}
C_l h^d \left(|\mathbf{v}_\Omega|^2 + |\mathbf{v}_\Gamma|^2 \right) &\leq \|\hat{\boldsymbol{v}}_h\|_{0,\Omega}^2 < C_u h^d \left(|\mathbf{v}_\Omega|^2 + |\mathbf{v}_\Gamma|^2 \right), \\
C_l h^d \left(|\mathbf{v}_\Gamma|^2 + |\mathbf{v}_\omega|^2 \right) &\leq \|\hat{\boldsymbol{v}}_h\|_{0,\omega}^2 < C_u h^d \left(|\mathbf{v}_\Gamma|^2 + |\mathbf{v}_\omega|^2 \right),
\end{aligned}
$$

where the bars $|\cdot|$ denote the two-norm of column vectors. Moreover, for quasi-uniform mesh families the following inverse estimates also hold [7, Thm. 4.5.11]: there is a constant C_I such that for $h \in (0, 1]$,

$$
(9.7) \quad
\begin{aligned}
h^2 |\boldsymbol{v}_h|_{1,\Omega}^2 &\leq C_I \|\boldsymbol{v}_h\|_0^2, \\
h^2 |\boldsymbol{v}_h|_{1,\omega}^2 &\leq C_I \|\boldsymbol{v}_h\|_0^2.
\end{aligned}
$$

Now we may estimate the stiffness matrix quadratic form as follows.

LEMMA 9.1. *Assuming that the mesh family associated with finite-element problem* (5.15) *is quasi uniform, there are μ_1, $\mu_2 > 0$ such that the corresponding system matrix $\mathbf{A}_\epsilon$ satisfies*

$$
(9.8) \quad \mu_1 h^d \left(|\mathbf{v}_\Omega|^2 + (1+\epsilon) |\mathbf{v}_\Gamma|^2 + \epsilon |\mathbf{v}_\omega|^2 \right) \leq \mathbf{v}^T \mathbf{A}_\epsilon \mathbf{v}
$$
$$
\leq \mu_2 h^{d-2} \left(|\mathbf{v}_\Omega|^2 + (1+\epsilon) |\mathbf{v}_\Gamma|^2 + \epsilon |\mathbf{v}_\omega|^2 \right)
$$

for any column vector $\mathbf{v}$ with the partitioning (9.3) *and for $\epsilon \in [0, 1/2]$.*

Proof. Let $\hat{\boldsymbol{v}}_h \in \hat{\boldsymbol{V}}$, and let $\mathbf{v}$ be the corresponding column vector of nodal values. By property (9.5) and definition (5.5a), we have

$$
(9.9) \quad
\begin{aligned}
\mathbf{v}^T \mathbf{A}_\epsilon \mathbf{v} = a_\epsilon(\boldsymbol{v}_h, \boldsymbol{v}_h) &= \int_\Omega \nabla \boldsymbol{v}_h \cdot \boldsymbol{E} \nabla \boldsymbol{v}_h + \epsilon \int_\omega \nabla \boldsymbol{v}_h \cdot \boldsymbol{E} \nabla \boldsymbol{v}_h \\
&\leq C_2 \left(|\boldsymbol{v}_h|_{1,\Omega}^2 + \epsilon |\boldsymbol{v}_h|_{1,\omega}^2 \right) \leq C_2 C_I h^{-2} \left(\|\boldsymbol{v}_h\|_{0,\Omega}^2 + \epsilon \|\boldsymbol{v}_h\|_{0,\omega}^2 \right) \\
&\leq C_2 C_I C_u h^{d-2} \left(|\mathbf{v}_\Omega|^2 + (1+\epsilon) |\mathbf{v}_\Gamma|^2 + \epsilon |\mathbf{v}_\omega|^2 \right),
\end{aligned}
$$

where the first inequality follows from continuity property (4.4), the second from inverse estimates (9.7), and the third from equivalence property (9.6). On the other hand, we have

$$
(9.10) \quad
\begin{aligned}
\mathbf{v}^T \mathbf{A}_\epsilon \mathbf{v} = a_\epsilon(\boldsymbol{v}_h, \boldsymbol{v}_h) &= \int_\Omega \nabla \boldsymbol{v}_h \cdot \boldsymbol{E} \nabla \boldsymbol{v}_h + \epsilon \int_\omega \nabla \boldsymbol{v}_h \cdot \boldsymbol{E} \nabla \boldsymbol{v}_h \\
&\geq C \left(\|\boldsymbol{v}_h\|_{1,\Omega}^2 + \epsilon \|\boldsymbol{v}_h\|_{1,\omega}^2 \right) \geq C \left(\|\boldsymbol{v}_h\|_{0,\Omega}^2 + \epsilon \|\boldsymbol{v}_h\|_{0,\omega}^2 \right) \\
&\geq C C_l h^d \left(|\mathbf{v}_\Omega|^2 + (1+\epsilon) |\mathbf{v}_\Gamma|^2 + \epsilon |\mathbf{v}_\omega|^2 \right),
\end{aligned}
$$

where the first inequality follows from Lemma 5.1 and the third from equivalence property (9.6). Together, inequalities (9.9) and (9.10) yield the claim with $\mu_1 = C C_l$ and $\mu_2 = C_2 C_I C_u$. $\square$

The estimates of Lemma 9.1 suggest the introduction of the diagonal scaling matrix

$$
(9.11) \quad \mathbf{D}_\epsilon = \mathrm{diag}(\mathbf{I}_{N_\Omega}, (1+\epsilon)\mathbf{I}_{N_\Gamma}, \epsilon \mathbf{I}_{N_\omega});
$$

that is, the first N_Ω diagonal elements of $\mathbf{D}_\epsilon$ are unity, the next N_Γ elements are $1+\epsilon$, and the last N_ω elements are ϵ. Using this scaling matrix, we may write

$$
(9.12) \quad |\mathbf{v}_\Omega|^2 + (1+\epsilon) |\mathbf{v}_\Gamma|^2 + \epsilon |\mathbf{v}_\omega|^2 = \mathbf{v}^T \mathbf{D}_\epsilon \mathbf{v}.
$$

THEOREM 9.2. *Assuming that the mesh family associated with finite-element problem* (5.15) *is quasi uniform, there is a constant C such that for $\epsilon \in (0, 1/2]$ and $h \in (0, 1]$, the stiffness matrix $\mathbf{A}_\epsilon$ associated with finite-element problem* (5.15) *satisfies*

$$
(9.13) \qquad
\begin{aligned}
\kappa(\mathbf{A}_\epsilon) &\leq Ch^{-2}\epsilon^{-1}, \\
\kappa(\mathbf{D}_\epsilon^{-1}\mathbf{A}_\epsilon) &\leq Ch^{-2},
\end{aligned}
$$

where $\mathbf{D}_\epsilon$ is the scaling matrix defined in expression (9.11).

Proof. Let $\mathbf{M}$ be an Nd-by-Nd symmetric and positive definite matrix. Recall that the maximum and minimum value of the generalized Rayleigh quotient

$$
(9.14) \qquad \psi(\mathbf{v}) = \frac{\mathbf{v}^T\mathbf{A}_\epsilon\mathbf{v}}{\mathbf{v}^T\mathbf{M}\mathbf{v}}
$$

among all $\mathbf{v} \neq \mathbf{0}$ are the maximum and minimum eigenvalues to the generalized eigenvalue problem

$$
(9.15) \qquad \mathbf{A}_\epsilon\mathbf{v} = \lambda\mathbf{M}\mathbf{v}.
$$

Thus, the quotient between upper and lower bounds of ψ yields an estimate of the spectral condition number $\mathbf{M}^{-1}\mathbf{A}$.

By its definition in expression (9.11), scaling matrix $\mathbf{D}_\epsilon$ satisfies

$$
(9.16) \qquad \epsilon|\mathbf{v}|^2 \leq \mathbf{v}^T\mathbf{D}_\epsilon\mathbf{v} \leq |\mathbf{v}|^2
$$

for each column vector $\mathbf{v}$ and for $\epsilon \in (0, 1/2]$. Lemma 9.1, expression (9.12), and the bounds (9.16) yield that there are $\mu_1, \mu_2 > 0$ such that

$$
(9.17) \qquad \mu_1 h^d\epsilon|\mathbf{v}|^2 \leq \mu_1 h^d\mathbf{v}^T\mathbf{D}_\epsilon\mathbf{v} \leq \mathbf{v}^T\mathbf{A}_\epsilon\mathbf{v} \leq \mu_2 h^{d-2}\mathbf{v}^T\mathbf{D}_\epsilon\mathbf{v} \leq \mu_2 h^{d-2}|\mathbf{v}|^2
$$

for each $\mathbf{v}$, from which we conclude that, for each nonzero $\mathbf{v}$,

$$
(9.18) \qquad \mu_1\epsilon h^d \leq \frac{\mathbf{v}^T\mathbf{A}_\epsilon\mathbf{v}}{|\mathbf{v}|^2} \leq \mu_2 h^{d-2}, \qquad \mu_1 h^d \leq \frac{\mathbf{v}^T\mathbf{A}_\epsilon\mathbf{v}}{\mathbf{v}^T\mathbf{D}_\epsilon\mathbf{v}} \leq \mu_2 h^{d-2}.
$$

The conclusion, with $C = \mu_2/\mu_1$, then follows from the max/min principle for eigenvalues discussed above. $\quad\square$

Recall that Theorem 8.3 shows that the numerical solution $\boldsymbol{u}_h^\epsilon$, obtained using stiffness matrix $\mathbf{A}_\epsilon$, approaches the exact solution $\boldsymbol{u}$ as $h, \epsilon \to 0$. Theorem 9.2 shows, however, that the convergence as $\epsilon \to 0$ is thwarted by increasing ill conditioning of $\mathbf{A}_\epsilon$, which is not surprising, since the equations associated with nodes inside ω vanish as $\epsilon \to 0$. A perhaps more surprising result of Theorem 9.2 is that the dependency on ϵ in the condition number disappears when using the preconditioned stiffness matrix

$$
(9.19) \qquad \tilde{\mathbf{A}}_\epsilon = \mathbf{D}_\epsilon^{-1}\mathbf{A}_\epsilon.
$$

In fact, the limit problem is also well defined, as we now show.

THEOREM 9.3. *The limit as $\epsilon \to 0$ of the preconditioned stiffness matrix $\tilde{\mathbf{A}}_\epsilon$ in expression* (9.19) *is the stiffness matrix of the elastically extended finite-element problem* (6.8) *with $\alpha = 1$.*

Proof. Let $\epsilon > 0$. The elements of stiffness matrix $\mathbf{A}_\epsilon$ are given by

$$
(9.20) \qquad \mathbf{e}_i^T\mathbf{A}_\epsilon\mathbf{e}_j = \int_\Omega \nabla\boldsymbol{\phi}_i \cdot \boldsymbol{E}\nabla\boldsymbol{\phi}_j + \epsilon\int_\omega \nabla\boldsymbol{\phi}_i \cdot \boldsymbol{E}\nabla\boldsymbol{\phi}_j.
$$

Let $\mathbf{e}_i$ be the ith column of the dN-by-dN identity matrix. From expression (9.20) and by definition (9.11), we see that that the element of the preconditioned matrix can be written

$$
\begin{aligned}
&\mathbf{e}_i^T \mathbf{D}_\epsilon^{-1} \mathbf{A}_\epsilon \mathbf{e}_j \\
(9.21) \quad &=
\begin{cases}
\displaystyle\int_\Omega \nabla\phi_i \cdot \boldsymbol{E}\nabla\phi_j + \epsilon \int_\omega \nabla\phi_i \cdot \boldsymbol{E}\nabla\phi_j = \int_\Omega \nabla\phi_i \cdot \boldsymbol{E}\nabla\phi_j & \text{for } i \in \mathcal{N}(\Omega), \\[2ex]
\displaystyle\frac{1}{1+\epsilon}\int_\Omega \nabla\phi_i \cdot \boldsymbol{E}\nabla\phi_j + \frac{\epsilon}{1+\epsilon}\int_\omega \nabla\phi_i \cdot \boldsymbol{E}\nabla\phi_j & \text{for } i \in \mathcal{N}(\Gamma), \\[2ex]
\displaystyle\epsilon^{-1}\int_\Omega \nabla\phi_i \cdot \boldsymbol{E}\nabla\phi_j + \int_\omega \nabla\phi_i \cdot \boldsymbol{E}\nabla\phi_j = \int_\omega \nabla\phi_i \cdot \boldsymbol{E}\nabla\phi_j & \text{for } i \in \mathcal{N}(\omega),
\end{cases}
\end{aligned}
$$

where the second equalities on the right side follow from the fact that the support of ϕ_i is contained in Ω and ω for i in $\mathcal{N}(\Omega)$ and $\mathcal{N}(\omega)$, respectively. For $i = 1, \ldots, dN$, define the basis functions $\tilde{\phi}_i^\epsilon$ by

$$
(9.22) \qquad \tilde{\phi}_i^\epsilon =
\begin{cases}
\phi_i & \text{for } i \in \mathcal{N}(\Omega \cup \omega), \\[2ex]
\left(\dfrac{1}{1+\epsilon}\chi_\Omega + \dfrac{\epsilon}{1+\epsilon}\chi_\omega\right)\phi_i & \text{for } i \in \mathcal{N}(\Gamma),
\end{cases}
$$

where χ_Ω and χ_ω are the characteristic functions on Ω and ω. Using definition (9.22), expression (9.21) can be written

$$
(9.23) \qquad \mathbf{e}_i^T \tilde{\mathbf{A}}_\epsilon \mathbf{e}_j = \mathbf{e}_i^T \mathbf{D}_\epsilon^{-1} \mathbf{A}_\epsilon \mathbf{e}_j = \int_{\hat\Omega} \nabla\tilde{\phi}_i^\epsilon \cdot \boldsymbol{E}\nabla\phi_j.
$$

We notice that $\tilde{\phi}_i^\epsilon$ and thus the right side of (9.23) are well defined also for $\epsilon = 0$, so $\tilde{\mathbf{A}}_\epsilon$ is thus well defined in the limit $\epsilon \to 0$. Moreover, by comparing the expression for $\tilde{\phi}_i^\epsilon$ with basis functions $\tilde{\phi}_i$ defined in expression (6.7), we note that $\tilde{\phi}_i^0 = \tilde{\phi}_i$, and thus that $\lim_{\epsilon \to 0} \tilde{\mathbf{A}}_\epsilon$ yields the stiffness matrix of the extended finite element problem (6.8) with $\alpha = 1$. $\quad\square$

Remark 9.4. The h^{-2} condition number bound of $\mathbf{D}_\epsilon^{-1}\mathbf{A}_\epsilon$ in Theorem 9.2 is the expected conditioning of a matrix associated with a finite-element discretization of second-order elliptic boundary-value problems.

10. Numerical experiments. To affirm the error estimate in Theorem 8.3 and the condition number bounds in Theorem 9.2, we perform numerical experiments by assuming that the domain with two holes shown in Figure 10.1 is filled with a homogeneous and isotropic material in a state of plane strain. The values $\nu = 0.29$ and $E = 1$ are used for Poisson's ratio and Young's modulus, respectively. Moreover, the traction $\boldsymbol{t} = (0, -1)^\mathsf{T}$ is applied to the right boundary. We solve problem (4.1) on the fine triangulation shown in Figure 10.1 using P_3 Lagrangian elements, and we denote its solution with $\boldsymbol{u}_{\mathrm{ref}}$. Note that no weak material approximation is used when computing the solution $\boldsymbol{u}_{\mathrm{ref}}$. To solve the approximated weak material problem (5.4), stiffness matrices $\int_\Omega \nabla\phi_i \cdot \boldsymbol{E}\nabla\phi_j$ and $\int_\omega \nabla\phi_i \cdot \boldsymbol{E}\nabla\phi_j$ are computed by FreeFem++ (http://www.freefem.org/ff++/) using P_1 Lagrangian elements and imported into GNU Octave, in which both the preconditioned and unpreconditioned problems are solved. The preconditioned problem is the one used when performing the error-estimate experiments.
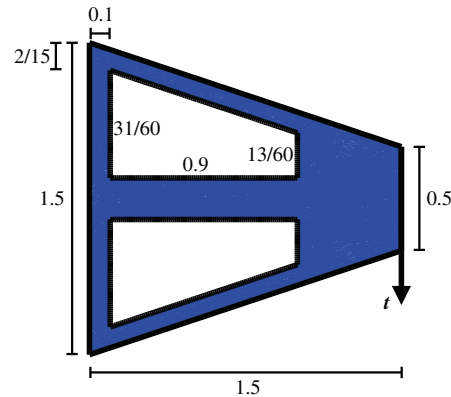
FIG. 10.1. *Domain Ω, triangulated with the mesh ($h \approx 0.015$) used to obtain the reference solution $\boldsymbol{u}_{ref}$.*
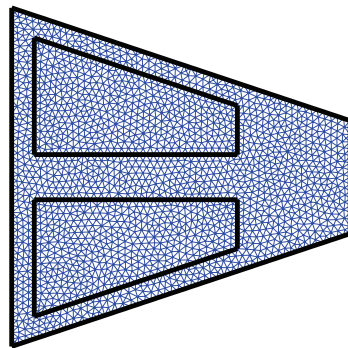

FIG. 10.2. *The extended domain $\hat{\Omega}$, triangulated with the mesh (Mesh I, $h \approx 0.082$) used to compute the numerical solution $\boldsymbol{u}_h^\epsilon$.*

Figure 10.3 depicts the seminorm error $|\boldsymbol{u}_{\text{ref}} - \boldsymbol{u}_h^\epsilon|_{1,\Omega}$ as a function of ϵ for three meshes with $h \approx 0.082$ (Mesh I), $h \approx 0.045$ (Mesh II), and $h \approx 0.026$ (Mesh III). Mesh I is depicted in Figure 10.2. We note that the error is not very sensitive to the value of ϵ, a conclusion that is in line with the experience of topology optimization practitioners, as noted in the introduction. The behavior of the error is consistent with the estimate of Theorem 8.3. For large ϵ, the error is dominated by the presence of the weak material and is independent of h. For $\epsilon \leq 10^{-4}$, the error is dominated by the approximation error term $O(h)$ associated with P_1 elements. In the region $10^{-2} \leq \epsilon \leq 10^{-3}$, the slope of the error curve in Figure 10.3 depends on the mesh in a manner consistent with the presence of two terms $O(h\epsilon^{1/2}) + O(\epsilon)$ as in the bound of Theorem 8.3. For the finest mesh, the slope approaches $O(\epsilon)$, whereas for the cruder mesh, the slope is less steep. Our experiments thus confirm a coupling between the finite-element and weak material errors of the type proven in Theorem 8.3, and we conclude that in order to avoid dominance of the $O(\epsilon^{1/2})$ term, sufficiently fine meshes have to be used.

Figure 10.4 visualizes the dependence of condition numbers $\kappa(\mathbf{A}_\epsilon)$ and $\kappa(\mathbf{D}_\epsilon^{-1}\mathbf{A}_\epsilon)$ on the weak material parameter ϵ. The solid lines indicate experiments performed using the three meshes without the preconditioner, whereas the lines marked with
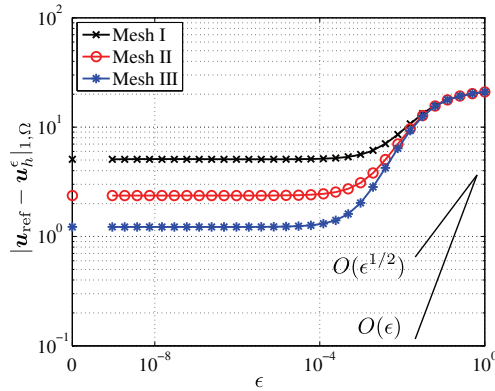
FIG. 10.3. *The $H^1(\Omega)$ seminorm error as a function of ϵ for three meshes. The preconditioner is used to compute $\boldsymbol{u}_h^\epsilon$. The isolated points to the left indicate the error for the limit problem $\epsilon \to 0$.*
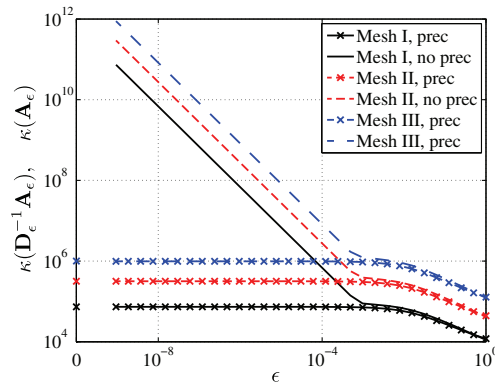

FIG. 10.4. *The condition number of the nonpreconditioned (lines) as well as the preconditioned (lines and crosses) stiffness matrices as a function of the weak material parameter ϵ. The isolated points to the left indicate the condition numbers for the limit problem $\epsilon \to 0$ when using the preconditioner.*

crosses indicate experiments using the preconditioner. We see that the condition number of matrix $\mathbf{A}_\epsilon$ grows inversely proportional to ϵ. Matrix $\mathbf{A}_0$ is not admissible since the solution inside the holes becomes undetermined. However, as also shown in Theorems 9.2 and 9.3, we see that the condition number of $\tilde{\mathbf{A}}_\epsilon$ is bounded independent of ϵ, and that $\tilde{\mathbf{A}}_0 \stackrel{\text{def}}{=} \lim_{\epsilon \to 0} \tilde{\mathbf{A}}_\epsilon$ is admissible with the bounded condition numbers shown on the κ-axis in Figure 10.4. As can be seen from Figures 10.3 and 10.4, in order to obtain a solution in which the effect of the weak material approximation is overshadowed by the finite-element error, the weak material parameter ϵ has to be less than 10^{-4}, which in the absence of the preconditioner results in a ill-conditioned coefficient matrix $\mathbf{A}_\epsilon$.

REFERENCES

[1] W. ACHTZIGER, *Multiple-load truss topology and sizing optimization: Some properties of minimax compliance*, J. Optim. Theory Appl., 98 (1998), pp. 255–280.

[2] G. ALLAIRE, *Shape Optimization by the Homogenization Method*, Appl. Math. Sci. 146, Springer, New York, 2002.

[3] M. P. BENDSØE AND N. KIKUCHI, *Generating optimal topologies in structural design using a homogenization method*, Comput. Methods Appl. Mech. Engrg., 71 (1988), pp. 197–224.

[4] M. P. BENDSØE AND O. SIGMUND, *Topology Optimization. Theory, Methods, and Applications*, Springer, New York, 2003.

[5] T. BORRVALL, *Topology optimization of elastic continua using restriction*, Arch. Comput. Methods Engrg., 8 (2001), pp. 351–385.

[6] D. BRAESS, *Finite Elements. Theory, Fast Solvers, and Applications in Solid Mechanics*, Cambridge University Press, Cambridge, UK, 2001.

[7] S. C. BRENNER AND L. R. SCOTT, *The Mathematical Theory of Finite Element Methods*, 2nd ed., Springer, New York, 2002.

[8] J. CÉA, A. GIOAN, AND J. MICHEL, *Quelques resultats sur l'identification de domaines*, Calcolo, 10 (1973), pp. 207–232.

[9] H. FREDRICSON, T. JOHANSEN, A. KLARBRING, AND J. PETERSSON, *Topology optimization of frame structures with flexible joints*, Struct. Multidiscip. Optim., 25 (2003), pp. 199–214.

[10] R. GLOWINSKI AND T.-W. PAN, *Error estimates for fictitious domain/penalty/finite element methods*, Calcolo, 29 (1992), pp. 125–141.

[11] R. GLOWINSKI, T. W. PAN, R. O. WELLS, JR., AND X. ZHOU, *Wavelet and finite element solutions for the Neumann problem using fictitious domains*, J. Comput. Phys., 126 (1996), pp. 40–51.

[12] P. GRISVARD, *Elliptic Problems in Non-Smooth Domains*, Pitman, London, 1985.

[13] M. E. GURTIN, *An Introduction to Continuum Mechanics*, Academic Press, New York, 2003.

[14] A. KLARBRING, J. PETERSSON, B. TORSTENFELT, AND M. KARLSSON, *Topology optimization of flow networks*, Comput. Methods Appl. Mech. Engrg., 192 (2003), pp. 3909–3932.

[15] L. KROG, A. TUCKER, M. KEMP, AND R. BOYD, *Application of topology, sizing and shape optimization methods to optimal design of aircraft components*, in Proceedings of the 4th Altair Technology Conference, 2004. Available online from http://www.altairhyperworks.co.uk/technology/papers/2004/Paper6.

[16] J. PETERSSON, *On continuity of the design-to-state mappings for trusses with variable topology*, Internat. J. Engrg. Sci., 39 (2001), pp. 1119–1141.

[17] A. QUARTERONI AND A. VALLI, *Numerical Approximation of Partial Differential Equations*, Springer Ser. Comput. Math. 23, Springer, Berlin, 2008.

[18] M. STOLPE AND K. SVANBERG, *On the trajectories of penalization methods for topology optimization*, Struct. Multidiscip. Optim., 21 (2001), pp. 128–139.

[19] M. STOLPE AND K. SVANBERG, *On the trajectories of the epsilon-relaxation approach for stress-constrained truss topology optimization*, Struct. Multidiscip. Optim., 21 (2001), pp. 140–151.

[20] K. SVANBERG AND M. WERME, *On the validity of using small positive lower bounds on design variables in discrete topology optimization*, Struct. Multidiscip. Optim., 37 (2009), pp. 325–334.

[21] J. WLOKA, *Partial Differential Equations*, Cambridge University Press, Cambridge, UK, 1987.

[22] S. ZHANG, *A domain embedding method for mixed boundary value problems*, C. R. Acad. Sci. Paris Sér. I Math., 343 (2006), pp. 287–290.